

## Adsorption of Fe(II) and Mn(II) using glauconitic greensands from aqueous solution

Dariush Naghipour<sup>a</sup>, Ramin Arjmand Movarrekh<sup>a</sup>, Kamran Taghavi<sup>a</sup>, Jalil Jaafari<sup>b,\*</sup>

<sup>a</sup>Department of Environmental Health Engineering, School of Health, Guilan University of Medical Sciences, Rasht, Iran, Tel. +98 131 3229599; Fax: +98 131 3234155; email: dnaghipour@yahoo.com (D. Naghipour), Tel. +989113329587; emails: raminarjmand98@gmail.com (R.A. Movarrekh), user37@gums.ac.ir (K. Taghavi)

<sup>b</sup>Research Center of Health and Environment, Guilan University of Medical Sciences, Rasht, Iran, Tel. +98 131 3234155; email: Jalil.Jaafari@yahoo.com (J. Jaafari)

Received 21 June 2019; Accepted 15 February 2020

---

### ABSTRACT

In this study, removing Fe(II) and Mn(II) through adsorption on greensand along with changes in the contact time, initial concentrations of the adsorbent, Fe(II) and Mn(II) and pH in a batch system was investigated. Also, results obtained from the experiment conducted on Freundlich and Langmuir isotherms and pseudo-first and second-order kinetic models were studied. Results showed that the removal efficiency of the adsorbent decreased to pH and iron/manganese concentrations increased. On the other hand, it increased with an increase in the primary concentration of the adsorbent and the contact time. Maximum adsorption for both adsorbents at pH 5 was achieved and adsorption capacity of the glauconitic greensand for Fe(II) and Mn(II) were 11.5 and 11.8 mg/g, respectively. Obtained results from equilibrium studies revealed that Fe(II) and Mn(II) adsorption process on the adsorbent followed the pseudo-second-order kinetic and Langmuir and Freundlich's isotherm models. In all, the experiment results indicated that the adsorption process on glauconite could be used as an effective method for removing Fe(II) and Mn(II) in aqueous solutions.

*Keywords:* Greensand (glauconite); Iron; Manganese; Kinetic model; Isotherm model; Adsorption

---

### 1. Introduction

Iron is the fourth abundant element that composes about 5% of the earth's crust. Iron contamination appears in two forms: ferric and ferrous. In surface waters, iron is often found as ferric, while in underground waters, it exists in the form of ferrous (soluble iron). Naturally, iron is insoluble and consists of solid particles [1,2]. In Freshwaters, its content is around 0.5–5 mg/L. Iron levels of more than 0.3 mg/L in water cause the taste to become undesirable, change the water color into red, leave stains on objects and clothing and also cause precipitation in water pipes and iron bacteria to grow in the water system [3–5]. The growth of these bacteria

in the drinking water causes odor, wells could be clogged and their systems would dysfunction and as a result, water supply decreases [6]. Up to the present, different processes such as aeration, oxidation, and ion exchange have been used to remove iron from drinking water resources.

Manganese is one the most abundant elements in the earth's crust which along with iron exists in most of the soils. Most often, it is found in the form of dioxide, carbonate, and silicate [7,8]. Manganese oxide in the form of Mn(II) and Mn(IV) is very important in a drinking water system [9]. At the moment, manganese ion is found in the slops of many industrial factories such as dry battery, glass, ceramic, paint, and safety match manufacturing companies and it is

---

\* Corresponding author.

also found as a catalyst in petrochemical industries. Water flowing through rocks that contain this metal can transfer it to groundwaters as well [10]. Conventional amounts of manganese in freshwaters are often in the 1–200 µg/L range. In 2012, World Health Organization recommended the concentration of manganese in the drinking water to be 0.1 mg/L and reminded that its 0.05–0.1 mg/L concentrations are acceptable for most consumers; however, in the long run, they would cause black sediments to be formed inside water-supplying pipes [11]. The concentration of Fe and Mn in the surface water is commonly less than 1 mg/L but in groundwater can be reached to higher than 1 mg/L. In the study of the assessment of Fe and Mn in groundwater in Tabriz, these concentrations were 965 and 425 µg/L [12]. In aqueous solutions, Mn(II) can affect the lives of humans and aquatic beings [13]. High concentrations of Mn(II) in the human body can damage the brain and lead to complications in the nervous system [14]. Some of the Mn(II) removing techniques include chemical precipitation [15], membrane filtration [16], adsorption of activated carbon [17], ion exchange [18], etc. Among these methods, adsorption has been widely used.

Up to the present, numerous research has been done on removing Fe(II) and Mn(II) both in Iran and throughout the world. For example, Outram et al. [19] concluded that through a filtration and adsorption mechanism, greensand beds could trap manganese. The efficiency of this mechanism would depend on parameters such as the volume of water, the speed of the water flow, contact time, the depth of the bed, etc. [3,20–23]. In 2013, Alslaiibi et al. [24] concluded that the efficiency of removing iron using carbon, obtained from olive pits, was 99.39% and that the second-order kinetics and adsorption isotherm followed the Langmuir model with an adsorption capacity of 57.47 mg/g. The objective of this study was to examine the ability of greensand in removing Fe(II) and Mn(II) from water.

Glauconite is the active substance in greensand. It belongs to the illite group of clay minerals and is a green mineral soil with ion-exchange property. It actually consists of hydrated aluminosilicate with a uniformity coefficient less than 1.6, a special mass of 2.5–2.9 kg/m<sup>3</sup> and 16–60 mesh, which can help water treatment through adsorption and oxidation. Glauconite is a suitable environment for reducing soluble pollutants in raw water resources, while the substance itself is not used in the removal process. Also, Glauconite was used as an adsorbent for adsorption of many pollutants such as: Pb(II), Zn(II) [25] U(VI), and Th(IV) [26]. Therefore, it has an economic advantage over other removal methods [2,20].

## 2. Materials and methods

### 2.1. Preparation of the adsorbent (Greensand)

In this research, the adsorbent (greensand) was gained from a local river with a large deposit. In order to separate the needed grain size, it was sifted using a laboratory sifter. Therefore, 18–40 mesh with a uniformity coefficient of 1.6 were separated and after being rinsed with abundant distilled water to remove external contamination and then, dried at 40°C, were prepared for the next stages [27]. To determine the physical characteristics of the adsorbent, a scanning electron

microscope (SEM) model LEO 1430VP (a joint product of Germany and England) was used, while for determining the compounds and structural particulars of the adsorbent, an X-ray diffraction device (XRD) model GNR-MPD3000 (manufactured in Italy) and an X-ray fluorescence device model ARL-8410 (manufactured in the USA) were used.

### 2.2. Adsorption study

Adsorption of Fe(II) and Mn(II) on greensand (Glauconite) was studied in a batch environment. To prepare the initial Fe(II) and Mn(II) concentrations, a stock solution (1,000 mg/L) of the two elements (Merck Co., Germany) was used and to adjust the pH, titrisol chloridric acid, and sodium hydroxide (Merck Co., Germany) were used. The primary and final analysis of Fe(II) and Mn(II) (after being centrifuged at 2,000 rpm) was performed using a spectrophotometer device UV/VIS model DR5000 (HACH company, Shanghai) at 510 and 445 nm wavelengths equal to the standard method No. 3500B [28]. The efficiency of Fe(II) and Mn(II) removal from the aqueous solution, was calculated using:

$$\text{Removal efficiency (\%)} = \frac{C_0 - C_e}{C_e} \times 100 \quad (1)$$

where  $C_0$  is the initial concentration (mg/L),  $C_e$  is the equilibrium concentration (mg/L).

The study of kinetics was done separately in a 250 mL Erlenmeyer flask containing 100 mL of Fe(II) and Mn(II) solution with each of the initial concentrations 0.2, 1, 2.5, 5, and 10 mg/L and pH 5 at 25°C for 2 h. Then, samples were separated and analyzed and the adsorption capacity was determined using Eq. (2).

$$q_e = \frac{(C_0 - C_e)V}{M} \quad (2)$$

where  $q_e$  is the adsorption capacity (mg/g),  $C_0$  is the initial concentration (mg/L),  $C_e$  is the equilibrium concentration (mg/L),  $V$  was the volume of the solution (mL), and  $M$  was the mass of the adsorbent [29,30].

The equilibrium test was performed separately in a 250 mL Erlenmeyer flask containing 100 mL of iron and manganese solution with each of the initial concentrations 0.2 to 10 mg/L, a primary amount of the adsorbent 1 g/L and pH 5 on an 80 rpm shaker at 25°C for 2 h.

The effect of contact time on the efficiency of removing Fe(II) and Mn(II) was measured in 2–120 min time, pH 5 with an 80 rpm shaker at 25°C with the initial concentrations of Fe(II) and Mn(II) in the range 0.2–10 mg/L.

The effect of pH on the efficiency of Fe(II) and Mn(II) removal was studied by changing the initial pH value from 3 to 11 using chloridric acid and sodium hydroxide at constant initial concentrations of Fe(II) and Mn(II) being 2.5 and 5 mg/L, respectively with the initial concentration of the adsorbent being 1 g/L at 25°C. The initial and final pH (after contact with the adsorbent at the time of equilibrium) were measured using a pH meter Model WTW-Multilane, Germany. The effect of the initial concentration of Fe(II) and Mn(II) on the removal efficiency in the studied system was

investigated by changing the initial concentrations of 0.2–10 mg/L of Fe(II) and Mn(II) at the constant pH 5 and the initial concentration of the adsorbent being 1 g/L on an 80 rpm shaker at 25°C. The effect of adsorbent amount on Fe(II) and Mn(II) removal efficiency was investigated on an 80 rpm shaker at 25°C by changing the adsorbent amount from 0.175 to 1 g/L at the constant pH 5 and the initial concentrations of Fe(II) and Mn(II), 2.5 and 5 mg/L, respectively.

### 3. Results and discussion

#### 3.1. Adsorbent characterization

The compounds and structural particulars of the adsorbent, greensand (Glaucanite), are shown in Fig. 1 and Table 1 as XRD patterns. Physical characteristics of the adsorbent are shown in Fig. 2 using SEM. As Fig. 1, porous surface morphology was showed in SEM result of greensand (Glaucanite). Chemical and mineralogical analysis of the greensand glaucanite presented in Table 1 indicated that glaucanite mainly consists of silica, ferric oxide,

and alumina with a ratio of SiO<sub>2</sub> to Al<sub>2</sub>O<sub>3</sub> while the ratio of SiO<sub>2</sub> to Fe<sub>2</sub>O<sub>3</sub> was around 2.5 and 2.3, in used glaucanite, respectively [31,32]. The raw glaucanite also including Na<sup>+</sup>, K<sup>+</sup>, Ca<sup>2+</sup>, Fe<sup>3+</sup>, Al<sup>3+</sup>, Ti<sup>2+</sup>, and Mg<sup>2+</sup> in decreasing magnitudes (wt.%), as a point to in Table 1 [27].

The XRD pattern of glaucanite showed the presence of quartz and dolomite. Also showing several diagnostic peaks around the area 2θ = 5°–10° represents within is the hexagonal crystal, and the peak observed several branches in the 2θ = 35°–38° and 5°–25° of glaucanite indicates that percentage is expected and presented accordance references [33]. The micro/mesostructure and surface morphology play a vital role in knowing the presence of pores in the pollutant adsorption capacity of glaucanite. The morphology of samples is shown in Fig. 2. The micrograph of glaucanite in Fig. 2 shows that the glaucanites are aggregated mass of irregular shape particles with the construction of illite-shaped, formed by several flaky particles that have great discontinuities and

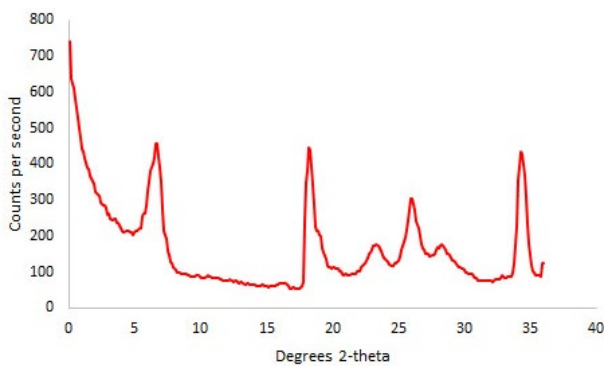


Fig. 1. XRD patterns of glaucanite.

Table 1  
Chemical composition of greensand

Component	Content%
SiO <sub>2</sub>	38.1
Fe <sub>2</sub> O <sub>3</sub>	16.5
Al <sub>2</sub> O <sub>3</sub>	15
CaO	10.8
MgO	4.1
Na <sub>2</sub> O	3
K <sub>2</sub> O	1.1
TiO <sub>2</sub>	2.2
P <sub>2</sub> O <sub>5</sub>	0.9
L.O.I	8.31

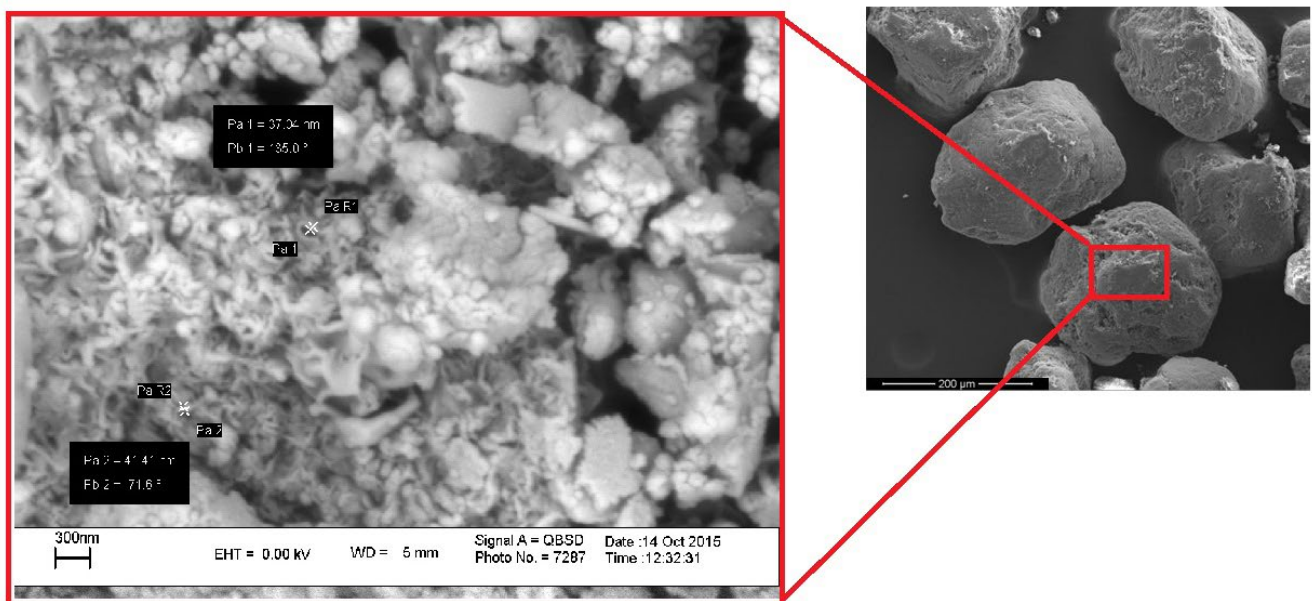


Fig. 2. SEM images of greensand (Glaucanite).

porosity [27,31,34]. According to Üzümlü et al. [35], the BET analysis shows the specific surface area and mean pore diameter of the glauconite were measured to be 11 21.2 m<sup>2</sup>/g, and 25 nm, respectively. The pH at the potential of zero point charge (pH<sub>zpc</sub>) of the glauconite was 7.7, and this matter confirmed that the adsorbing surface in different pH is under 7.7 is positive and higher than it is negative.

### 3.2. Effect of contact time on the adsorption capacity

Figs. 3a and b show the effect of contact time on Fe(II) and Mn(II) adsorption capacity. As shown in the figures, when the contact time increased from 2 to 60 min, iron adsorption capacity increased from 0.83 to 4.21 (mg/g) (initial concentration of 5 mg/L) and manganese adsorption capacity increased from 0.89 to 4.39 (mg/g) (initial concentration of 5 mg/L), respectively. Therefore, the equilibrium time for Fe(II) and Mn(II) was found to be 60 min [24].

The highest level of Fe(II) and Mn(II) removal was done at the first 0–30 min after which the removal process had a constant trend with a slight increase. A probable reason could be that at the initial stage, the number of available adsorption sites was more, and the propulsion for transferring the adsorbed substance was greater [36,37]. Therefore, the adsorbed part was more easily connected to adsorption sites. With the passage of time, the number of active sites decreased and they got captured by the adsorbed substance [38–40]. So, its entrance became limited and time-consuming [21,41–43]. These results were consistent with those obtained in studies conducted by Gogoi et al. [44].

There are different models of adsorption kinetics including first order, pseudo-first-order, and pseudo-second-order of adsorption. In this study, pseudo-first and second-order kinetics were used for obtaining the results (Fig. 4). Pseudo-first-order kinetics can be expressed in Eq. (3).

$$\ln\left(1 - \frac{q_t}{q_e}\right) = -k_1 \times t \quad (3)$$

where  $q_e$  and  $q_t$  are the amounts of the adsorbed substance (mg/g) at equilibrium and  $t$  time, and  $k_1$  is the constant of

speed (l/min). As a whole, pseudo-second-order kinetics can be expressed in Eq. (4).

$$\frac{t}{q_t} = \frac{1}{k_2 q_e^2} + \frac{1}{q_e} \times t \quad (4)$$

In this equation,  $k_2$  is the constant of speed (g/mg min). By drawing  $t/q_e$  against the contact time,  $k_2$  and  $q_e$  values could be obtained using gradient and width from the matrix in the curve above. Parameters of kinetics studies are given in Table 2.

With  $R^2$  correlation coefficients taken into consideration, it could be concluded that adsorption data followed the pseudo-second-order kinetics. The pseudo-second-order kinetics for Fe(II) and Mn(II) are shown in Figs. 3a and b, respectively.

### 3.3. Effect of pH on Fe(II) and Mn(II) removal efficiency

The effect of pH on the removal efficiency is shown in Fig. 5. As seen, removal efficiency due to adsorption increased with an increase in pH up until pH 5 and for Fe(II) and Mn(II), the values in 120 min in initial concentration of Fe(II) 2.5 mg/L and Mn(II) 10 mg/L were 84.8%, 67.4% at pH 3 and 82.4%, 87.5% at pH 5, respectively. When pH value increased from 5 to 11, the efficiency of Fe(II) and Mn(II) adsorption decreased, reaching 54% and 20%, respectively.

Changes in the efficiency of removing Fe(II) and Mn(II) upon variations in the pH value could be interpreted based on the pH<sub>zpc</sub> of the adsorbent, the form of Fe(II) and Mn(II) mold at the said pH value and the surface charge of the adsorbent at different pH values. Upon hydration, hydroxyl groups are formed on the adsorbent's surface [45,46]. These hydroxyl groups have buffer properties which are (Al, Fe, Si) OH<sub>2</sub><sup>+</sup>, (Al, Fe, Si) OH, and (Al, Fe, Si) O<sup>-</sup> positive, negative, and neutral groups on the surface of glauconite pH<sub>zpc</sub> is a 7.6 adsorbent. It affirms the fact that the surface charge of the adsorbent at pH less than 7.6 is positive and at higher pH, it's negative. Low efficiency of the adsorption of Fe(II) and Mn(II) in acidic conditions can be due to the competitive effect of positive hydrogen ions with soluble cations on the two elements—though the number of positive hydrogen

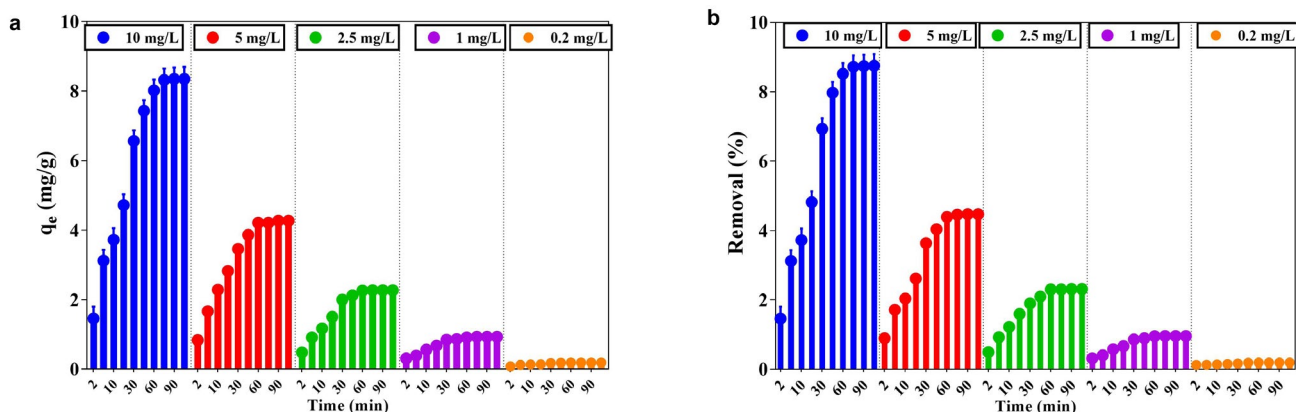


Fig. 3. Effect of contact time on Fe(II) (a) and Mn(II) adsorption capacity by greensand (b) (pH: 5, greensand 1 g/L).

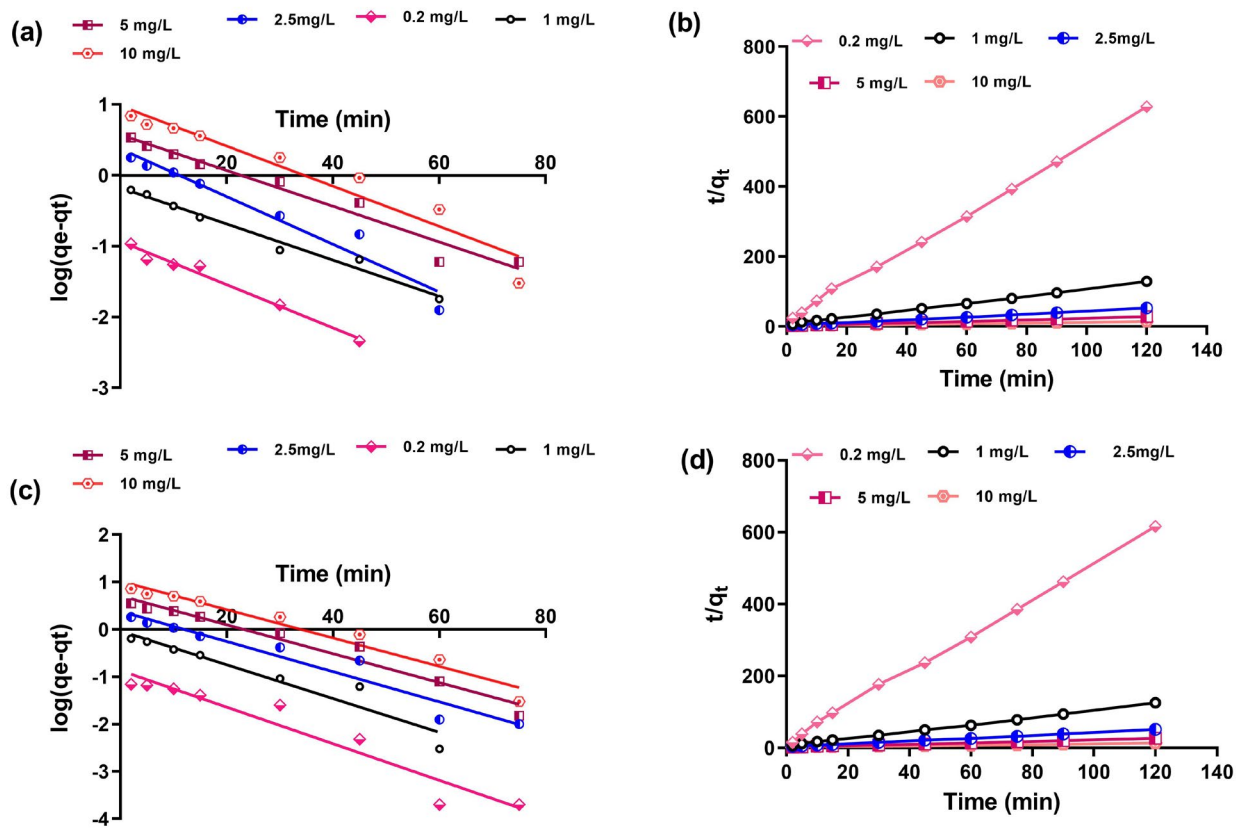


Fig. 4. Pseudo-first and second-order kinetic for Fe(II) (a and b) and Mn(II) removal by greensand (c and d) (greensand 1 g/L, pH: 5).

Table 2  
Kinetic parameters for adsorption rate expression

Element	C <sub>0</sub> (mg/L)	q <sub>e</sub> (exp)	Pseudo-first-order equation			Pseudo-second-order equation		
			k <sub>1</sub>	q <sub>e</sub> (mg/g)	R <sup>2</sup>	k <sub>2</sub>	q <sub>e</sub> (mg/g)	R <sup>2</sup>
Fe(II)	0.2	0.19	0.07	0.12	0.98	1.3	0.2	0.996
	1	0.93	0.05	0.65	0.98	0.15	1	0.996
	2.5	2.27	0.059	2.37	0.94	0.047	2.48	0.996
	5	4.27	0.058	3.76	0.97	0.02	4.68	0.997
	10	8.35	0.06	9.59	0.992	0.008	9.39	0.99
Mn(II)	0.2	0.19	0.08	0.14	0.88	1.48	0.2	0.994
	1	0.95	0.08	0.93	0.91	1.5	1.02	0.995
	2.5	2.31	0.07	2.42	0.89	0.04	2.53	0.996
	5	4.47	0.07	5.12	0.96	0.01	4.98	0.98
	10	8.75	0.069	10.46	0.98	0.008	9.92	0.98

ions decreases upon an increase in the pH value, the number of positive-charged Fe(II) and Mn(II) cations increases [47]. Therefore, the higher the pH value, the more the number of hydrogen ions decreases and the efficiency of removing Fe(II) and Mn(II) increases as well. However, the reduction trend of the removal efficiency at pH higher than 5 could be attributed to using caustic soda (NaOH) to increase pH, where Fe(II) and Mn(II) cations bind to OH<sup>-</sup> and heavily precipitate and cause the adsorption efficiency to decrease.

These results are consistent with those of Zhang et al. [48]. Fig. 5 shows the pattern for pH changes in determining the surface pH in greensand. Results indicate that greensand has a buffering property.

### 3.4. Effect of glauconite dose on the removal efficiency

The effect of the glauconite dose on Fe(II) and Mn(II) removal efficiency is shown in Fig. 6. As the initial glauconite

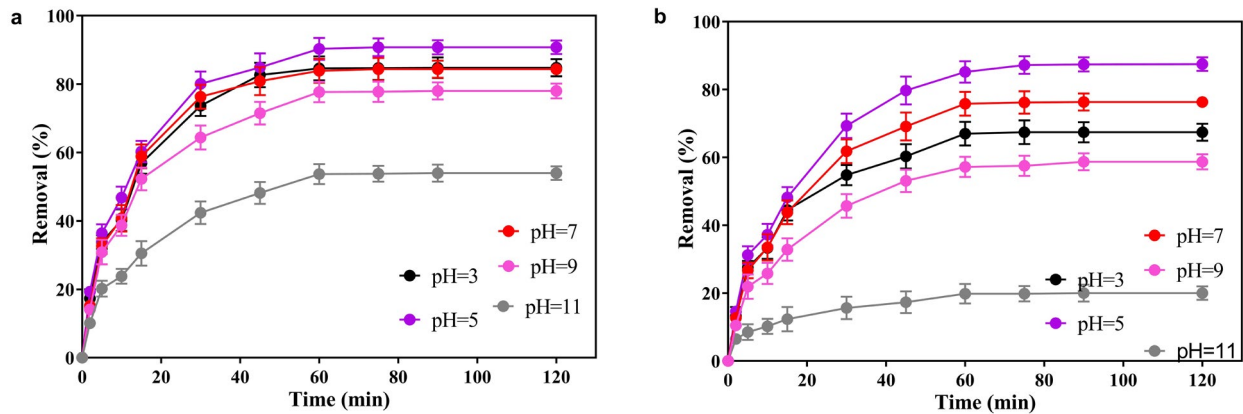


Fig. 5. Effect of pH on Fe(II) (a) and Mn(II) (b) removal efficiency (Fe(II): 2.5 mg/L, Mn(II): 10 mg/L, greensand 1 g/L).

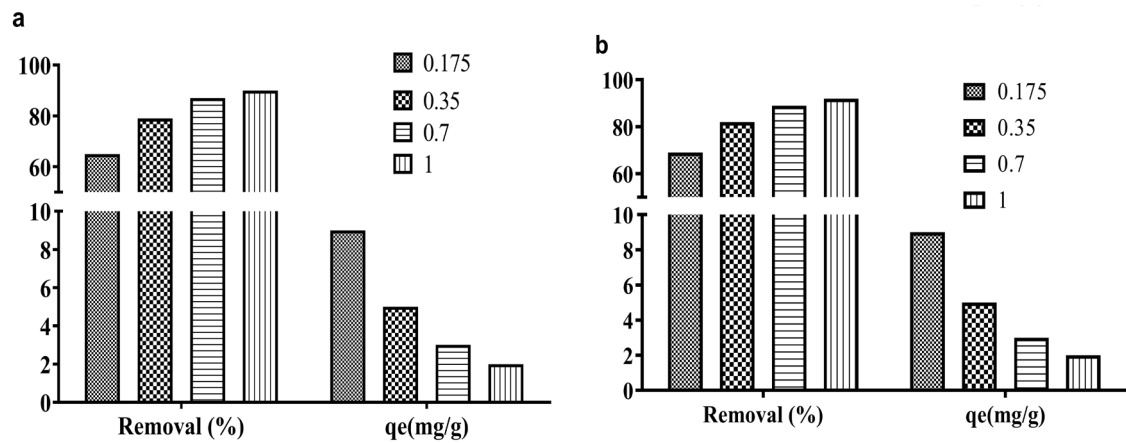


Fig. 6. Effect of glauconite dose on Fe(II) (a) and Mn(II) (b) removal capacity and adsorption capacity of the greensand.

dose increased, removal efficiency decreased in a way that when the glauconite dose increased from 0.175 to 1 g/L, the removal efficiency increased from 65.5% and 69.8% to 90.8% and 92.5%, also adsorption capacity ( $q_e$ ) decreased from 9.4% and 9.9% to 2.2 and 2.3 (mg/g), respectively [49]. Adsorption of Fe(II) and Mn(II) increased as the amount of greensand (Glauconite), as an adsorbent, increased which could be due to increased active adsorption sites or a general increase in the special adsorption surface for cations which existed in the environment. These results are consistent with those of [50].

Iron and manganese ions removal using the adsorbent decreased as the initial concentrations increased. The reason was that adsorbents have limited active sites which in high pollutant concentrations, are saturated rapidly and thus, cause the adsorbent's efficiency to decrease. Adsorption isotherms are equations for describing the equilibrium between solid and liquid phases of the adsorbed part. The empirical data of the adsorption equilibrium with Freundlich and Langmuir models of adsorption isotherms were studied in this research.

The Langmuir isotherm model is valid in terms of monolayer adsorption. The linear form of Langmuir isotherm model is given in Eq. (5).

$$\frac{C_e}{q_e} = \frac{C_e}{q_m} + \frac{1}{b \times q_m} \quad (5)$$

where  $q_e$  is the amount of the adsorbed substance per mass unit of the adsorbent in equilibrium (mg/g),  $C_e$  is the equilibrium concentration of the adsorbed substance in a solution after adsorption (mg/L),  $q_m$  is the maximum amount of the adsorbed substance per mass unit for the adsorbent at equilibrium (mg/g), and  $b$  is the Langmuir constant. Langmuir isotherm model for the present study is shown in Fig. 7.

The linear form of Freundlich isotherm model is given in Eq. (6) [51]:

$$\log q_e = \log K_f + \frac{1}{n} \log C_e \quad (6)$$

where  $q_e$  is the amount of the substance adsorbed per mass unit at equilibrium (mg/g),  $C_e$  is the equilibrium concentration of the adsorbed substance in the solution after adsorption (mg/L), and  $K_f$  and  $n$  are Freundlich constants.

Tempkin considered the effect of some indirect sorbate/adsorbate interactions on the adsorption isotherm.

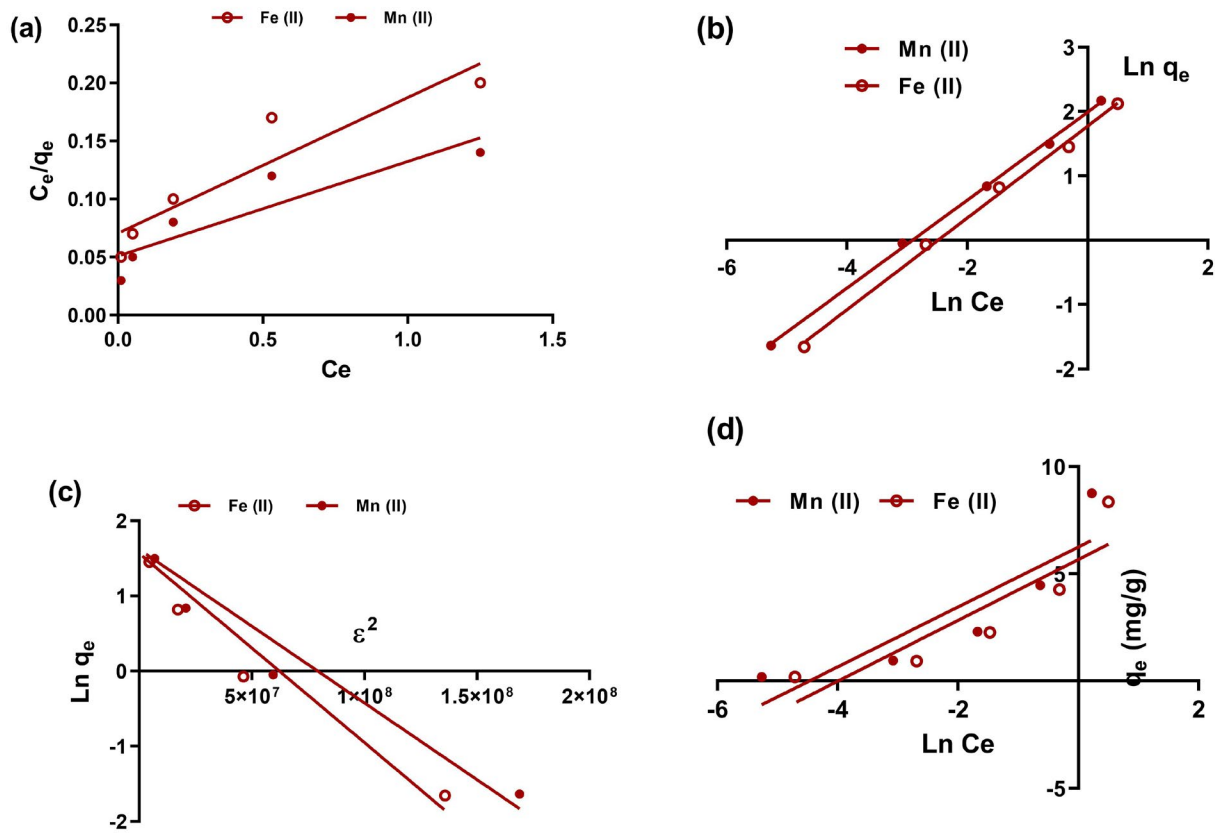


Fig. 7. The linearized (a) Langmuir, (b) Freundlich, (c) Dubinin–Radushkevich, and (d) Temkin adsorption isotherm for Fe(II) and Mn(II) adsorption.

This isotherm assumes that; the heat of adsorption of all the molecules in a layer decreases linearly with surface coverage of adsorbent due to sorbate–adsorbate interactions.

This adsorption is characterized by a uniform distribution of binding energies. The linear form of the Tempkin isotherm equation is represented by the following equation [38]:

$$q_e = B_1 \ln(k_i) + B_1 \ln(C_e) \tag{7}$$

where  $B = RT/b$ ,  $T$  is the absolute temperature in K,  $R$  the universal gas constant ( $8.314 \text{ K mol}^{-1}$ ),  $k_i$  is the equilibrium binding constant, and the constant  $B_1$  is related to the heat of adsorption.

Dubinin and Radushkevich have proposed another isotherm which is not based on the assumption of homogeneous surface or constant adsorption potential by the following equation:

$$\ln C_{\text{abs}} = \ln X_m - K\varepsilon^2 \tag{7}$$

where  $K$  and  $\varepsilon$  are Dubinin–Radushkevich isotherm constants. The saturation adsorption capacity  $q_m$  and  $K$  were calculated from the intercept and slope of  $\ln q_e$  vs.  $\varepsilon$ . In the present study, the isotherm models are shown in Fig. 7.

Adsorption isotherms are adsorption properties and equilibrium data which describe how pollutants react with adsorbents and how essential their role is in optimizing

the consumption of adsorbents. In other words, creating a suitable relationship for the equilibrium curve and optimizing an adsorption system for removing metal cations or other pollutants is very important. The parameters of the isotherm models are shown in Table 3. With the correlation coefficient  $R^2$  taken into account, equilibrium data for Fe(II) and Mn(II). Freundlich isotherm describes the

Table 3  
Adsorption isotherms tested

Isotherm	Parameter	Fe(II)	Mn(II)
Langmuir	$q_m$ (mg/g)	11.5	11.7
	$b$ (L/mg)	1.21	1.7
	$R^2$	0.85	0.83
Freundlich	$K_f$ (mg/g(L/mg) <sup>1/n</sup> )	59.2	97.7
	$n$	1.4	1.4
	$R^2$	0.996	0.998
Temkin	$k_i$ (L/mg)	0.083	0.06
	$B_1$	1.41	1.39
	$R^2$	0.79	0.77
Dubinin–Radushkevich	$q_m$ (mg/g)	4.78	5.02
	$\beta$	2.51	2.04
	$R^2$	0.91	0.91

Table 4  
Comparison of adsorption capacity of Fe(II) and Mn(II) onto various adsorbents

Adsorbents	Adsorption capacity (mg/g)	Initial Fe(II) concentration (mg/L)	Initial Mn(II) concentration (mg/L)	pH	Reference
Greensand	11.8		10	5	This study
Activated carbon	172		50	4	[52]
Bone char	22		100	6.5	[53]
Natural zeolite	6.96		200	3.5	[54]
	7.68		50	6	[55]
Calcined bentonite	0.5		50	5.3	[56]
Granular activated carbon	2		2	7	[57]
Metakaolin based geopolymer	72.3		100	3	[58]
Greensand	11.5	10		5	This study
Pecan shell-based activated carbon	41.6	55		3.5	[59]
Rice husk ash	6.2	40		6	[60]
Chitosan	64.1	6		5	[61]
Olive stone waste	57.4	50		5	[24]
Combretum quadrangulare Kurz AC	15.5	100		6	[62]
Pomegranate peel waste	18.5	100		6	[63]

adsorption process on heterogeneous surfaces. Therefore, the amount of adsorption energy is not the same in all adsorption sites for it to result in multi-layer adsorption needed for manganese. These results are consistent with those of Gogoi et al. [44].

### 3.5. Comparison with previous works

Comparison of different adsorbents and its capacity towards the adsorption of Fe(II) and Mn(II) utilized in the literature are given in Table 4. Based on the precursor material used, the adsorption capacities vary, mostly because of the differences in structures including inorganic porous material with immense structures area, natural and synthetic polymer. The adsorption of Fe(II) and Mn(II) from aqueous solution can be related to the pH of the solution because it affects the adsorbent surface charge, ionization degree, and adsorbent species. The solution aqueous phase pH governs the speciation of metals and also the dissociation of surface functional groups and preferential adsorption of ions. Similar studies have proven that the pH is an important variable affecting the metals adsorption partly because hydrogen ions can compete strongly with adsorbate metal ions for low pH active sites as well as the propensity of precipitation at high pH.

As shown in Table 4, Some of the adsorbent materials were higher adsorption capacity of Fe(II) and Mn(II) as compared to the results obtained in this work, for example, activated carbon, bone char, metakaolin based geopolymer for Mn(II) adsorption, and pecan shell-based activated carbon, chitosan, olive stone waste, Combretum quadrangulare Kurz activated carbon, for Fe(II) adsorption. This could be due to the excellent properties of these adsorbents such as high specific surface area and rich surface functional groups. But adsorption capacity in this study was higher than in natural zeolite, calcined bentonite, granular activated carbon for Mn(II), and rice husk ash for Fe(II) adsorption. Nevertheless,

this work generally shows that low-cost glauconite exhibits a comparable standing in Mn(II) and Fe(II) adsorption with some adsorbents found in the literature.

## 4. Conclusion

Results indicated that greensand had a relatively high capability in adsorption of Fe(II) and Mn(II) from aqueous solutions. The removal rate of Fe(II) and Mn(II) were the highest at pH 5. Adsorption kinetics followed the second-order model, while adsorption isotherm followed the Freundlich model for Fe(II) and Mn(II). Results suggest that greensand can be effectively used as the adsorbent for the removal of Fe(II) and Mn(II) ions from aqueous solution and should be investigated in future studies.

## Acknowledgments

This paper was supported financially by a grant (No. 93120416) from the Guilan University of Medical Sciences, Rasht, Iran.

## References

- [1] O. Ribolzi, E. Rochelle-Newall, S. Dittrich, Y. Auda, P.N. Newton, S. Rattanavong, M. Knappik, B. Souleleuth, O. Sengtaheuanghoung, D.A. Dance, Land use and soil type determine the presence of the pathogen *Burkholderia pseudomallei* in tropical rivers, *Environ. Sci. Pollut. Res.*, 23 (2016) 7828–7839.
- [2] F.N. Oskui, H. Aghdasinia, M.G. Sorkhabi, Adsorption of Cr(III) using an Iranian natural nanoclay: applicable to tannery wastewater: equilibrium, kinetic, and thermodynamic, *Environ. Earth Sci.*, 78 (2019) 106.
- [3] S.R. Qasim, E.M. Motley, G. Zhu, *Water Works Engineering: Planning, Design, and Operation*, Prentice Hall, 2000.
- [4] J. Jaafari, K. Yaghmaeian, Optimization of heavy metal biosorption onto freshwater algae (*Chlorella coloniales*) using response surface methodology (RSM), *Chemosphere*, 217 (2019) 447–455.

- [5] J. Jaafari, K. Yaghmaeian, Response surface methodological approach for optimizing heavy metal biosorption by the blue-green alga *Chroococcus disperses*, *Desal. Water Treat.*, 142 (2019) 225–234.
- [6] R. Saeedi, K. Naddafi, R. Nabizadeh, A. Mesdaghinia, S. Nasser, M. Alimohammadi, S. Nazmara, Simultaneous removal of nitrate and natural organic matter from drinking water using a hybrid heterotrophic/autotrophic/biological activated carbon bioreactor, *Environ. Eng. Sci.*, 29 (2012) 93–100.
- [7] H. Kamani, M. Hoseini, G.H. Safari, J. Jaafari, A.H. Mahvi, Study of trace elements in wet atmospheric precipitation in Tehran, Iran, *Environ. Monit. Assess.*, 186 (2014) 5059–5067.
- [8] H. Kamani, A. Mahvi, M. Seyedsalehi, J. Jaafari, M. Hoseini, G. Safari, A. Dalvand, H. Aslani, N. Mirzaei, S. Ashrafi, Contamination and ecological risk assessment of heavy metals in street dust of Tehran, Iran, *Int. J. Environ. Sci. Technol.*, 14 (2017) 2675–2682.
- [9] J.E. Post, Manganese oxide minerals: crystal structures and economic and environmental significance, *Proc. Natl. Acad. Sci. U. S. A.*, 96 (1999) 3447–3454.
- [10] A.K. Meena, G. Mishra, P. Rai, C. Rajagopal, P. Nagar, Removal of heavy metal ions from aqueous solutions using carbon aerogel as an adsorbent, *J. Hazard. Mater.*, 122 (2005) 161–170.
- [11] S.R. Taffarel, J. Rubio, On the removal of Mn<sup>2+</sup> ions by adsorption onto natural and activated Chilean zeolites, *Miner. Eng.*, 22 (2009) 336–343.
- [12] R. Barzegar, A.A. Moghaddam, N. Kazemian, Assessment of heavy metals concentrations with emphasis on arsenic in the Tabriz plain aquifers, Iran, *Environ. Earth Sci.*, 74 (2015) 297–313.
- [13] World Health Organization, Water, Sanitation, Health Team, Guidelines for Drinking-Water Quality [Electronic Resource]: Incorporating First Addendum, Vol. 1, Recommendations, 3rd ed., World Health Organization, Geneva, 2006.
- [14] R.J. Elsner, J.G. Spangler, Neurotoxicity of inhaled manganese: public health danger in the shower?, *Med. Hypotheses*, 65 (2005) 607–616.
- [15] J. Shu, R. Liu, Z. Liu, H. Chen, C. Tao, Simultaneous removal of ammonia and manganese from electrolytic metal manganese residue leachate using phosphate salt, *J. Cleaner Prod.*, 135 (2016) 468–475.
- [16] S.A. Aya, T. Ormanci Acar, N. Tufekci, Modeling of membrane fouling in a submerged membrane reactor using support vector regression, *Desal. Water Treat.*, (2016) 1–14.
- [17] L. Yang, X. Jiang, Z.-S. Yang, W.-J. Jiang, Effect of MnSO<sub>4</sub> on the removal of SO<sub>2</sub> by manganese-modified activated coke, *Ind. Eng. Chem. Res.*, 54 (2015) 1689–1696.
- [18] G. Coşkun, İ. Şimşek, Ö. Arar, Ü. Yüksel, M. Yüksel, Comparison of chelating ligands on manganese (II) removal from aqueous solution, *Desal. Water Treat.*, 57 (2016) 1–8.
- [19] J.G. Outram, S.J. Couperthwaite, G.J. Millar, Comparative analysis of the physical, chemical and structural characteristics and performance of manganese greensands, *J. Water Process Eng.*, 13 (2016) 16–26.
- [20] G.H. Safari, M. Zarrabi, M. Hoseini, H. Kamani, J. Jaafari, A.H. Mahvi, Trends of natural and acid-engineered pumice onto phosphorus ions in aquatic environment: adsorbent preparation, characterization, and kinetic and equilibrium modeling, *Desal. Water Treat.*, 54 (2015) 3031–3043.
- [21] D. Naghipour, K. Taghavi, J. Jaafari, Y. Mahdavi, M. Ghanbari Ghoskhal, R. Ameri, A. Jamshidi, A. Hossein Mahvi, Statistical modeling and optimization of the phosphorus biosorption by modified *Lemna minor* from aqueous solution using response surface methodology (RSM), *Desal. Water Treat.*, 57 (2016) 19431–19442.
- [22] M. Abtahi, A. Mesdaghinia, R. Saeedi, S. Nazmara, Biosorption of As(III) and As(V) from aqueous solutions by brown macroalga *Colpomenia sinuosa* biomass: kinetic and equilibrium studies, *Desal. Water Treat.*, 51 (2013) 3224–3232.
- [23] M. Pirsaeheb, M. Mohamadi, A.M. Mansouri, A.A.L. Zinatizadeh, S. Sumathi, K. Sharafi, Process modeling and optimization of biological removal of carbon, nitrogen and phosphorus from hospital wastewater in a continuous feeding & intermittent discharge (CFID) bioreactor, *Korean J. Chem. Eng.*, 32 (2015) 1340–1353.
- [24] T.M. Alslaibi, I. Abustan, M.A. Ahmad, A.A. Foul, Kinetics and equilibrium adsorption of iron (II), lead (II), and copper (II) onto activated carbon prepared from olive stone waste, *Desal. Water Treat.*, 52 (2014) 7887–7897.
- [25] K.A.-E. Selim, R.S. El-Tawil, N.A. Abdel-Khalek, Heavy metals removal using surface modified Glauconite mineral, *Int. J. Miner. Process. Extr. Metall.*, 1 (2016) 46–55.
- [26] O. Ali, H.H. Osman, S.A. Sayed, M.E. Shalabi, The removal of uranium and thorium from their aqueous solutions via glauconite, *Desal. Water Treat.*, 53 (2015) 760–767.
- [27] D. Naghipour, K. Taghavi, M. Ashournia, J. Jaafari, R. Arjmand Movarrek, A study of Cr(VI) and NH<sub>4</sub><sup>+</sup> adsorption using greensand (glauconite) as a low-cost adsorbent from aqueous solutions, *Water Environ. J.*, 34 (2020) 45–56.
- [28] WEF, APHA, Standard Methods for the Examination of Water and Wastewater, American Public Health Association (APHA), Washington, DC, USA, 2005.
- [29] F.N. Oskui, H. Aghdasinia, M.G. Sorkhabi, Modeling and optimization of chromium adsorption onto clay using response surface methodology, artificial neural network, and equilibrium isotherm models, *Environ. Prog. Sustainable Energy*, 38 (2019).
- [30] K. Naddafi, N. Rastkari, R. Nabizadeh, R. Saeedi, M. Gholami, M. Sarkhosh, Adsorption of 2,4,6-trichlorophenol from aqueous solutions by a surfactant-modified zeolitic tuff: batch and continuous studies, *Desal. Water Treat.*, 57 (2016) 5789–5799.
- [31] E. Derakhshani, A. Naghizadeh, Optimization of humic acid removal by adsorption onto bentonite and montmorillonite nanoparticles, *J. Mol. Liq.*, 259 (2018) 76–81.
- [32] S. Dobaradaran, R.N. Nodehi, K. Yaghmaeian, J. Jaafari, M.H. Niari, A.K. Bharti, S. Agarwal, V.K. Gupta, A. Azari, N. Shariatifar, Catalytic decomposition of 2-chlorophenol using an ultrasonic-assisted Fe<sub>3</sub>O<sub>4</sub>-TiO<sub>2</sub>@MWCNT system: influence factors, pathway and mechanism study, *J. Colloid Interface Sci.*, 512 (2018) 172–189.
- [33] I.E. Odom, Microstructure, mineralogy and chemistry of Cambrian glauconite pellets and glauconite, central USA, *Clays Clay Miner.*, 24 (1976) 232–238.
- [34] M. Kamranifar, A. Allahresani, A. Naghizadeh, Synthesis and characterizations of a novel CoFe<sub>2</sub>O<sub>4</sub>@CuS magnetic nanocomposite and investigation of its efficiency for photocatalytic degradation of penicillin G antibiotic in simulated wastewater, *J. Hazard. Mater.*, 366 (2019) 545–555.
- [35] Ç. Üzümlü, T. Shahwan, A.E. Eroğlu, K.R. Hallam, T.B. Scott, I. Lieberwirth, Synthesis and characterization of kaolinite-supported zero-valent iron nanoparticles and their application for the removal of aqueous Cu<sup>2+</sup> and Co<sup>2+</sup> ions, *Appl. Clay Sci.*, 43 (2009) 172–181.
- [36] M. Moradi, M. Soltanian, M. Pirsaeheb, K. Sharafi, S. Soltanian, A. Mozafari, The efficiency study of pumice powder to lead removal from the aquatic environment: isotherms and kinetics of the reaction, *J. Mazandaran Univ. Med. Sci.*, 23 (2014) 65–75.
- [37] M. Pirsaeheb, M. Moradi, H. Ghaffari, K. Sharafi, Application of response surface methodology for efficiency analysis of strong non-selective ion exchange resin column (A 400 E) in nitrate removal from groundwater, *Int. J. Pharm. Technol.*, 8 (2016) 11023–11034.
- [38] A. Naghizadeh, M. Ghafouri, Synthesis and performance evaluation of chitosan prepared from Persian gulf shrimp shell in removal of reactive blue 29 dye from aqueous solution (isotherm, thermodynamic and kinetic study), *Iran. J. Chem. Chem. Eng.*, 36 (2017) 25–36.
- [39] K. Naddafi, R. Saeedi, Biosorption of copper (II) from aqueous solutions by brown macroalga *Cystoseira myrica* biomass, *Environ. Eng. Sci.*, 26 (2009) 1009–1015.
- [40] S. Dobaradaran, I. Nabipour, M. Keshtkar, F.F. Ghasemi, T. Nazarialamdarloo, F. Khalifeh, M. Poorhosein, M. Abtahi, R. Saeedi, Self-purification of marine environments for heavy metals: a study on removal of lead (II) and copper (II) by cuttlebone, *Water Sci. Technol.*, 75 (2016) 474–481.
- [41] S.D. Ashrafi, H. Kamani, J. Jaafari, A.H. Mahvi, Experimental design and response surface modeling for optimization of

- fluoroquinolone removal from aqueous solution by NaOH-modified rice husk, *Desal. Water Treat.*, 57 (2016) 16456–16465.
- [42] S. Ashrafi, H. Kamani, H. Soheil Aezomand, N. Yousefi, A. Mahvi, Optimization and modeling of process variables for adsorption of Basic Blue 41 on NaOH-modified rice husk using response surface methodology, *Desal. Water Treat.*, 57 (2016) 14051–14059.
- [43] A. Dehghan, A. Zarei, J. Jaafari, M. Shams, A.M. Khaneghah, Tetracycline removal from aqueous solutions using zeolitic imidazolate frameworks with different morphologies: a mathematical modeling, *Chemosphere*, 217 (2019) 250–260.
- [44] D. Gogoi, A. Shanmugamani, S. Rao, T. Kumar, S. Velmurugan, Study of removal process of manganese using synthetic calcium hydroxyapatite from an aqueous solution, *Desal. Water Treat.*, 57 (2016) 6566–6573.
- [45] M. Pirsahab, Z. Rezai, A. Mansouri, A. Rastegar, A. Alahabadi, A.R. Sani, K. Sharafi, Preparation of the activated carbon from India shrub wood and their application for methylene blue removal: modeling and optimization, *Desal. Water Treat.*, 57 (2016) 5888–5902.
- [46] M. Moradi, A.M. Mansouri, N. Azizi, J. Amini, K. Karimi, K. Sharafi, Adsorptive removal of phenol from aqueous solutions by copper (Cu)-modified scoria powder: process modeling and kinetic evaluation, *Desal. Water Treat.*, 57 (2016) 11820–11834.
- [47] A.F. Taiwo, N.J. Chinyere, Sorption characteristics for multiple adsorption of heavy metal ions using activated carbon from Nigerian bamboo, *J. Chem. Eng. Mater. Sci.*, 4 (2016) 39–48.
- [48] W. Zhang, C.Y. Cheng, Y. Pranolo, Investigation of methods for removal and recovery of manganese in hydrometallurgical processes, *Hydrometallurgy*, 101 (2010) 58–63.
- [49] S.R. Taffarel, J. Rubio, Removal of Mn<sup>2+</sup> from aqueous solution by manganese oxide coated zeolite, *Miner. Eng.*, 23 (2010) 1131–1138.
- [50] N. Rajic, D. Stojakovic, S. Jevtic, N.Z. Logar, J. Kovac, V. Kaucic, Removal of aqueous manganese using the natural zeolitic tuff from the Vranjska Banja deposit in Serbia, *J. Hazard. Mater.*, 172 (2009) 1450–1457.
- [51] D. Balarak, Y. Mahdavi, F. Ghorzin, S. Sadeghi, Biosorption of acid blue 113 dyes using dried *Lemna minor* biomass, *Sci. J. Environ. Sci.*, 5 (2016) 152–158.
- [52] A. Omri, M. Benzina, Removal of manganese (II) ions from aqueous solutions by adsorption on activated carbon derived a new precursor: *Ziziphus spina-christi* seeds, *Alexandria Eng. J.*, 51 (2012) 343–350.
- [53] D.C. Sicupira, T.T. Silva, V.A. Leão, M.B. Mansur, Batch removal of manganese from acid mine drainage using bone char, *Braz. J. Chem. Eng.*, 31 (2014) 195–204.
- [54] A. Zendelska, M. Golomeova, K. Blažev, B. Boev, B. Krstev, B. Golomeov, A. Krstev, Kinetic studies of manganese removal from aqueous solution by adsorption on natural zeolite, *Maced. J. Chem. Chem. Eng.*, 34 (2015) 213–220.
- [55] A. Ates, Role of modification of natural zeolite in removal of manganese from aqueous solutions, *Powder Technol.*, 264 (2014) 86–95.
- [56] J.A. Alexander, M.A.A. Zaini, S. Abdulsalam, U. Aliyu El-Nafaty, U.O. Aroke, Isotherm studies of lead (II), manganese (II), and cadmium (II) adsorption by Nigerian bentonite clay in single and multimetal solutions, *Part. Sci. Technol.*, 37 (2019) 399–409.
- [57] M.E. Goher, A.M. Hassan, I.A. Abdel-Moniem, A.H. Fahmy, M.H. Abdo, S.M. El-Sayed, Removal of aluminum, iron and manganese ions from industrial wastes using granular activated carbon and Amberlite IR-120H, *Egypt. J. Aquat. Res.*, 41 (2015) 155–164.
- [58] I. Kara, D. Tunc, F. Sayin, S.T. Akar, Study on the performance of metakaolin based geopolymer for Mn(II) and Co(II) removal, *Appl. Clay Sci.*, 161 (2018) 184–193.
- [59] A.R. Kaveeshwar, S.K. Ponnusamy, E.D. Revellame, D.D. Gang, M.E. Zappi, R. Subramaniam, Pecan shell based activated carbon for removal of iron (II) from fracking wastewater: adsorption kinetics, isotherm and thermodynamic studies, *Process Saf. Environ. Prot.*, 114 (2018) 107–122.
- [60] Y. Zhang, J. Zhao, Z. Jiang, D. Shan, Y. Lu, Biosorption of Fe(II) and Mn(II) ions from aqueous solution by rice husk ash, *Biomed. Res. Int.*, 2014 (2014) 1–10.
- [61] W.W. Ngah, S. Ab Ghani, A. Kamari, Adsorption behaviour of Fe(II) and Fe(III) ions in aqueous solution on chitosan and cross-linked chitosan beads, *Bioresour. Technol.*, 96 (2005) 443–450.
- [62] P. Maneechakr, S. Karnjanakom, Adsorption behaviour of Fe(II) and Cr(VI) on activated carbon: surface chemistry, isotherm, kinetic and thermodynamic studies, *J. Chem. Thermodyn.*, 106 (2017) 104–112.
- [63] M.R. Moghadam, N. Nasirizadeh, Z. Dashti, E. Babanezhad, Removal of Fe(II) from aqueous solution using pomegranate peel carbon: equilibrium and kinetic studies, *Int. J. Ind. Chem.*, 4 (2013) 19.